Analytica Chimica Acta 1084 (2019) 53–59

Contents lists available at ScienceDirect

Analytica Chimica Acta

journal homepage: www.elsevier.com/locate/aca

Redesigning the T-probe for mass spectrometry analysis of online lysis of non-adherent single cells

Yanlin Zhu, Renmeng Liu, Zhibo Yang*

Department of Chemistry and Biochemistry, University of Oklahoma, 101 Stephenson Parkway, Norman, OK, 73019, USA

HIGHLIGHTS

- A microscale sampling and ionization device allows for MS analysis of suspended live single cells.
- Entire single cells underwent rapid online lysis without losing cellular contents.
- Metabolomic biomarkers and biological pathways were discovered at the single cell level.

GRAPHICAL ABSTRACT

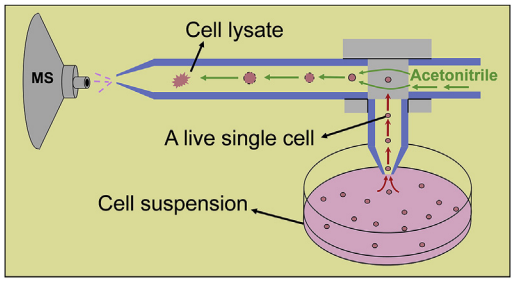

ARTICLE INFO

Article history:
Received 21 May 2019
Received in revised form
25 July 2019
Accepted 28 July 2019
Available online 31 July 2019

Keywords:
Single cell mass spectrometry
T-probe
Online cell lysis
Non-adherent single cell analysis
Single cell metabolomics

ABSTRACT

Single cell mass spectrometry (SCMS) allows for molecular analysis of individual cells while avoiding the inevitable drawbacks of using cell lysate prepared from populations of cells. Based on our previous design of the T-probe, a microscale sampling and ionization device for SCMS analysis, we further developed the device to perform online, and real time lysis of non-adherent live single cells for mass spectrometry (MS) analysis at ambient conditions. This redesigned T-probe includes three parts: a sampling probe with a small tip to withdraw a whole cell, a solvent-providing capillary to deliver lysis solution (i.e., acetonitrile), and a nano-ESI emitter in which rapid cell lysis and ionization occur followed by MS analysis. These three components are embedded between two polycarbonate slides and are jointed through a T-junction to form an integrated device. Colon cancer cells (HCT-116) under control and treatment (using anticancer drug irinotecan) conditions were analyzed. We detected a variety of intracellular species, and structural identification of selected ions was conducted using tandem MS (MS^2). We further conducted statistical analysis (e.g., PLS-DA and *t*-test) to gain biological insights of cellular metabolism. Our results indicate that the influence of anticancer drugs on cellular metabolism of live non-adherent cells can be obtained using the SCMS experiments combined with statistical data analysis.

1. Introduction

The basic structural, functional, and biological units of life are cells. Great efforts have been devoted in recent decades to study the dynamic nature of cells, and to understand their roles in complex biological systems [1,2]. However, a particular cell is an individual unit with unique genomic and phenotypic traits, and thus distinguishes itself from other seemingly identical cells that reside in adjacent regions [3]. Such phenomenon termed as cell-to-cell heterogeneity poses a great challenge for clinical and biological studies, as a majority of conventional methods are based on cell

* Corresponding author.
E-mail address: zhibo.yang@ou.edu (Z. Yang).

https://doi.org/10.1016/j.aca.2019.07.059
0003-2670/

populations, which result in averaged results of the cohort analyzed [4]. Facing such challenges, single cell based techniques that can differentiate such cell-to-cell heterogeneity are desired to gain insights into the nature of cells. Currently, a variety of studies at the single cell level have been conducted, and they have fundamentally enhanced our understandings of cells through single cell genomics [5], single cell transcriptomics [6], single cell proteomics [7], and single cell metabolomics [8]. These studies provide chemical and biological information of target systems that is otherwise lost in traditional analyses using samples prepared from bulk populations of cells [3]. Among those single cell "omics" approaches, single cell metabolomics focuses on changes of cellular metabolites corresponding to altered microenvironment, and thus provides direct clues towards cellular metabolism [9].

Mass spectrometry (MS), as a powerful analytical approach, satisfies prerequisites of single cell metabolomic analysis due to its abilities to analyze trace amount of samples, resolve cellular metabolites from complex matrix [10], and identify species of interest [11]. A variety of different single cell MS (SCMS) techniques, which fall into non-ambient or ambient method (i.e., non-ambient, ambient), according to their sampling and ionization environment, have been developed and applied to analyses of a broad range of cells (plant cells, mammalian cells, yeasts, etc.) [12–14].

Non-ambient SCMS methods are primarily based on two ionization techniques: secondary ion MS (SIMS) and matrix-assisted desorption/ionization (MALDI) MS. Techniques based on SIMS and MALDI MS use high-energy ion beams or UV laser to ablate and ionize molecules in cells, such as metabolites, lipids, and pharmaceuticals, for sensitive and reproducible analysis at the single cell level [13,15]. In contrast to vacuum-based techniques, ambient SCMS methods allow for sampling and ionization of cells with little or no sample preparation [16–18]. A variety of ambient SCMS techniques, such as live single-cell video-MS [19], laser ablation electrospray ionization (LAESI) MS [20], nanospray desorption electrospray ionization (nano-DESI) MS [21], induced nanoESI (InESI) MS [22], probe electrospray ionization (PESI) [23,24], and techniques coupled to microfluidic chips [25] and flow cytometry (i.e., mass cytometry) [26,27]. In addition, we have previously developed the Single-probe [28–31], which was also used for MS imaging [29,32–34] of tissues and MS analysis of extracellular molecules in live spheroids [35], and the T-probe [36] to capture chemical information of live single cells. These approaches hold promising potentials towards studies of fundamental cell biology and translational applications in clinical practice [12].

Due to the extremely small amount of contents from a single cell (e.g., a single cell volume can be as low as a few pLs, with a few types of cells being smaller than 1 pL) [37,38], sample separation, which can potentially result in analyte dilution and loss, is not performed in most SCMS methods. On the other hand, suitable separation techniques can be coupled to MS techniques to improve sensitivity and identification. These separation techniques include micro-separation prior to ionization (e.g., capillary electrophoresis [39] and microscale liquid chromatography [40,41]) and post-ionization (i.e., ion mobility separation [42]). These techniques have been applied to *in situ* metabolic analysis of single plant cells [43] and quantifying translational cell heterogeneity in the frog embryo [44].

Despite great efforts contributed, two major limitations still exist in most of SCMS techniques mentioned above. First, these methods require cell immobilization or attachment to a particular substrate [45]. Second, loss of cellular contents may occur during sample preparation or sampling processes. The former prevents sampling from inherently non-adherent cells, whereas the latter renders a loss of molecular information of cellular contents.

To address the above limitations, we provided a new design of the T-probe that enables rapid lysis of live non-adherent single cells followed by immediate MS analysis. This new design was based on our previously reported T-probe device [36]. They both have three capillaries (i.e., a solvent-providing capillary, a sampling probe, and a nano-ESI emitter) that are joint to form a T-shaped junction and sandwiched by two polycarbonate slides (Fig. 1B). The working mechanisms of both designs are similar. During the SCMS experiment, the sampling solvent is provided a solvent pump and delivered to the solvent-providing capillary, which is connected to a conductive union. A DC ionization voltage is applied on the conductive union and transmitted through the solvent inside the capillaries to generate ionization at the nano-ESI emitter. Under well-tuned conditions (e.g., suitable solvent flowrate and ionization voltage), a suction force can be generated at the sampling probe. Although the exact mechanisms are unclear, the generation of the suction force is likely due to the capillary action in the sampling probe induced by a continuous consumption of solvent in the nano-ESI emitter [36].

The novelty of the T-probe used in the current study includes two major aspects. First, it is designed for the analysis of suspension cells. Although the majority of existing SCMS techniques, including the T-probe device, only allow for analyzing cells attached to

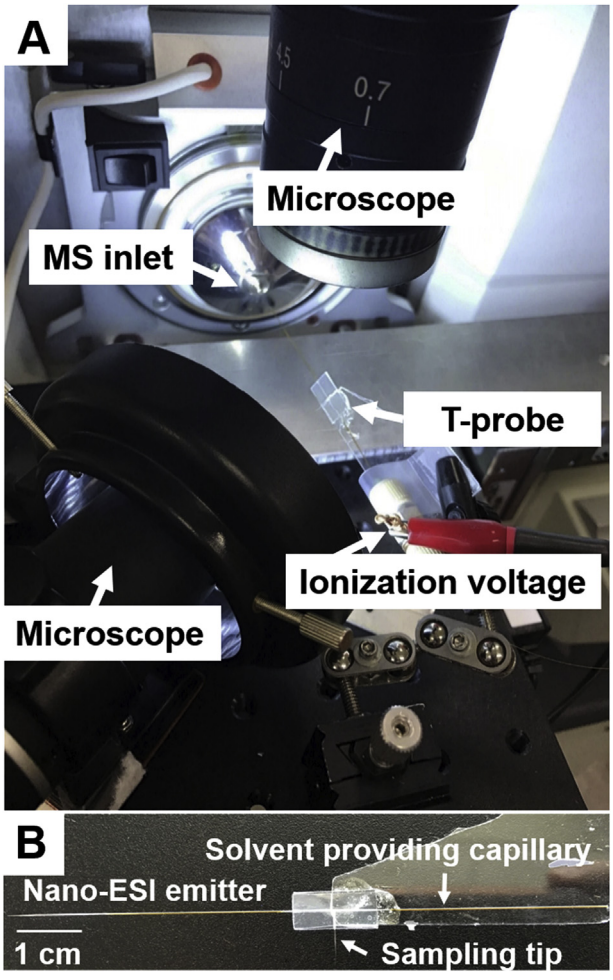

Fig. 1. (A) Experimental set-up of the redesigned T-probe for SCMS analysis. Two microscopes were used to provide visual guide during the experiment, and the XYZ-stage was utilized to precisely target single cells. Ionization voltage was applied on the conductive union, and the MS analysis was conducted using a LTQ Orbitrap XL mass spectrometer. (B) Photo of a T-probe, in which a solvent-providing capillary, a cell sampling probe, and a nano-ESI emitter were sandwiched by two polycarbonate slides.

substrates, methods based on mass cytometry [27], PESI [24] and microfluid chip devices [46] have been developed to analyze suspension cells. The capability of analyzing suspension cells is particularly important for clinical investigations, in which suspension cells, including primary blood cells (e.g., lymphocytes, macrophages, dendritic cells), lymph node cells (T-cells and B-cells), bone marrow cells, and circulating tumor cells, can be analyzed for cell-based therapy and diagnostics [47–50]. Our group has recently reported an integrated cell manipulation platform (ICMP) for MS analysis of single suspension cells [51]. Compared with this technique, the redesigned T-probe is a relatively simple device allowing for higher throughput analysis. Second, the new design allows for the analysis of an entire cell undergoing an online, rapid lysis. A cell can be withdrawn from the solution and followed by a rapid lysis inside the nano-ESI emitter of the device to avoid the loss of cellular contents, which can potentially occur during the sampling process of other techniques. Compared with the previously reported T-probe, the new design accordingly has two major features. First, because the new design aims to sample an entire non-adherent cell, its sampling probe has an orifice (~14 μm) slightly larger than that of the T-probe (~6 μm). Second, its nano-ESI emitter (5.5 cm) is much longer than that of the T-probe (~0.5 cm), allowing for adequate time (~15 s) to induce online cell lysis inside the nano-ESI emitter upon the cell contacting the solvent (99.9% acetonitrile with 0.1% formic acid (FA)) at the T-junction.

2. Experimental design and data processing

2.1. Fabrication and test of the T-probe

Although the general fabrication workflows of both designs are similar [36], the major differences between them include the length of nano-ESI emitter and tip size of sampling probe. The fabrication work is illustrated in Fig. S1, and detailed information is provided in the Support Information. Briefly, three capillaries (a solvent-providing capillary, a cell sampling probe, and a nano-ESI emitter) were joint at a T-shaped junction and sandwiched by two polycarbonate slides, which were coated with hydrophobic material and then bond together through a thermal binding process to form an integrated device (Fig. 2). We have conducted experiments using a series of tip sizes, and we selected a tip size of ~14 μm for both the sampling probe and the nano-ESI emitter to achieve the optimized performance. In addition, the lengths of the sampling probe (8 mm) and the nano-ESI emitter (5.5 cm) were carefully selected. Ideally, the length of the sampling probe should be short enough to minimize the amount of cell culture medium drawn along with a cell (i.e., minimized matrix effect) [10], but long enough to maintain a strong mechanical strength of the polycarbonate bond structure. On the other hand, with two major functions (i.e., online cell lysis and ionization) of the nano-ESI emitter, its length needs to be long enough to provide space and time for rapid cell lysis occurring upon the cell entering the T-junction and mixing with the solvent. However, an excessively long emitter can reduce the experimental throughput and result in difficulties of probe fabrication.

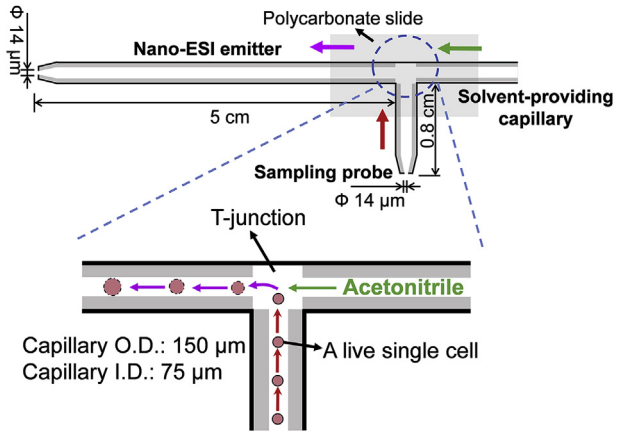

Fig. 2. Schematic of the T-probe and mechanisms of SCMS analysis. The inset shows the single cell withdrawn into the cell sampling probe undergoes a rapid (within a few seconds) lysis. Single cell lysate is immediately ionized through the nano-ESI emitter for MS analysis.

The performance of all devices was tested prior to the SCMS experiments. Simply, a small droplet of a prepared solution containing a standard testing compound (e.g., leucine enkephalin, 1 μM) was added to a vial, followed by immersion of the sampling probe tip into the solution. A stable ion signal of leucine enkephalin can be observed shortly (~15 s) after the probe immersion (Fig. S2). The sampling probe tip was then removed from the prepared solution, and the sampling solvent was continuously delivered to rinse the probe until the ion signal of the testing compound completely disappeared. To evaluate the sensitivity of the redesigned T-probe, we measured the limit of detection (LOD) of multiple standard compounds relevant to our studies. As a result, LODs were 0.1, 0.1, and 10 nM, for irinotecan, leucine enkephalin, and a phosphatidylcholine (PC (16:0/18:1)), respectively (Fig. S3). These results indicated that the new design has similar sensitivities compared with the original T-probe, the Single-probe, and standard nano-ESI source results [36,52]. (Table S1).

2.2. SCMS experiments

During the SCMS analysis, the redesigned T-probe was coupled to our in-home developed SCMS platform employed in our previous SCMS studies using the Single-probe [28,30,35] and the original T-probe [36]. Briefly, this platform includes an XYZ-translational stage system, two digital microscopes, and a Thermo LTQ Orbitrap XL mass spectrometer (Fig. 1A) [28]. Cells in both control and drug treatment groups were used for the SCMS experiments (detailed sample preparation procedures are described in the Supporting Information). Irinotecan is a common anticancer drug for the treatment of colon cancer [53] that inhibits the function of *Topoisomerase I*, leading to DNA damage and cell apoptosis [53,54]. This drug compound was selected to treat live HCT-116 colorectal cells in our experiments to demonstrate the change of cellular metabolites upon the treatment of anticancer agent. Specifically, cells were first treated using 18 μM irinotecan for 45 min, and then rinsed and detached using trypsinization. Afterwards, a droplet of cell suspension solution was placed onto a glass slide, which was attached to the XYZ-stage system controlled by a LabView software package (incremental step size = 0.1 μm) [55]. Using two digital microscopes as the visual guide, the sampling probe tip initially located above the sample plate was submerged into the solution containing cells by lifting the Z-stage. Upon selecting a target cell, the sampling probe can precisely draw the target cell with visual guidance (Fig. S4). The XYZ-stage was then immediately lowered down to free the sampling probe tip from the culture medium and stop the suction of culture medium. Due to the complex composition of the cell culture medium that may affect the detection sensitivity [10], caution should be taken to minimize its amount withdrawn during cell sampling. This is particularly important for future analysis of patient cells suspended in complex biological fluids such as blood, urine, saliva, and cerebrospinal fluid (CSF). After a single cell was withdrawn, the solvent provided through the solvent-providing capillary (flowrate = 0.5 μL/min) mixed with the

cell at the T-junction, and cell lysis rapidly occurred inside the nano-ESI emitter. In our SCMS analysis, an ionization voltage (+4 kV) was applied to the conductive union and transmitted throughout the solution inside the solvent-providing capillary and the nano-ESI emitter to ionize the cell lysis for MS analysis.

2.3. SCMS data analysis

A comprehensive data analysis procedure was performed following SCMS analysis to gain biological insights. Specifically, we conducted data pre-treatment, including removal of background (i.e., species detected in the sampling solvent, the culture medium, and any dissolved polycarbonate oligomers), reduction of instrumental noise, ion signal normalization, and peak alignment (see the Supporting Information and Fig. S5 for details) [56]. We performed statistical analyses, including Partial Least Squares-discriminant Analysis (PLS-DA) and two-sample *t*-test (hereinafter referred to as *t*-test), using an online metabolomics analysis tool, MetaboAnalyst [57]. PLS-DA is a multivariate statistical method for data analysis and visualization, and it has been widely applied to classification and regression of metabolomics data [58]. In addition, *t*-test is generally used to determine if there is a statistically significant difference between results from two groups of cells. In our work, we employed both methods to study the change of cellular metabolomic profiles upon drug treatment. Furthermore, two online metabolome databases, METLIN [59] and HMDB [60], were used to tentatively assign the detected metabolites based on their accurate *m/z* values. More confident identification of species of interest was performed using MS/MS fragmentation patterns.

3. Results and discussion

3.1. Sampling solvent selection

A key feature of the new design of the T-probe is to induce a rapid cell lysis during the transport of a cell from the T-junction to the tip of the nano-ESI emitter. It is critical to select MS-compatible solvents with desired composition for the SCMS experiments. To rapidly screen the solvent composition to be used in the SCMS analysis for optimal performance, we used a microscope (Micromaster, Fisher Scientific, MA) to monitor the lysis process of HCT-116 cells upon adding the lysis solution. A number of solvents commonly used in MS experiments (e.g., acetonitrile, methanol, and methanol/water) with a variety of compositions were tested as the lysis solution (Table 1). Our experiments indicated that cell lysis rapidly occurred (<15 s) in solution containing high concentrations of acetonitrile (>80%) (Fig. S6). Considering that a small amount of culture media would also be drawn along with a cell into the T-probe and therefore dilute the concentration of cellular contents, we used a sampling solvent composed of pure acetonitrile (with 0.1% FA to improve ionization efficiency) for our SCMS experiments.

Table 1
Influence of solvent composition (acetonitrile/cell culture medium) on cell lysis rate.

Percentage of acetonitrile (%)	Cell lysis rate (s)
20	>120
40	>60
60	≥60
80	10–15
90	<3
95	<3

3.2. Molecular analysis of single cells in the control and drug treatment groups

During the SCMS analysis, the ion signals of cellular species were usually observed within 15 s upon the selected cell entering the sampling probe tip. We analyzed 25 cells in the control group and 19 cells in the drug treated group, and a total number of ~400 cellular metabolites were detected (Fig. 3). As expected, irinotecan ($[C_{33}H_{38}N_4O_6 + H]^+$, *m/z* 587.2881) was only detected in the drug treated cells. By accomplishing the tentative assignment of detected species, we found that cellular species detected in the control group include phosphatidylcholine (PC), metabolites of vitamin D_3, phosphatidylethanolamide (PE), prostaglandin (PG), and PE-ceramide (PE-cer). For cells in the drug treated group, PC, PG, and PE were the major species. The forms of the detected species include protonated, sodiated, and potassiated species. Furthermore, the ion signal of one cell usually lasted for 15–20 s, which was adequate to conduct MS/MS analysis of a selected ion with relatively higher abundance (e.g., $>10^5$) at the single cell level. Among all abundant cellular species (e.g., top 30 most abundant species in the control and treatment groups), six of them were further identified by MS/MS analysis at the single cell level (Tables S2 and S3, Fig. S7 and Fig. S8). However, the signal intensities of the rest species were inadequate for MS/MS analysis at the single cell level due to multiple factors, including very limited amount of cellular contents, the ionization suppression by salts (from cell culture medium), and pronounced background signals. Therefore, we used traditional nanoESI-MS/MS to analyze cell lysate samples as a complimentary method (see the Support Information for detailed procedures of the lysate preparation and MS analysis). For example, the identification of irinotecan has been confirmed by MS/MS analysis in single cells (Fig. S7), cell lysate (Fig. S10), and the standard irinotecan solution. In addition, five cellular species were detected in both control and drug treatment groups, and they were identified as PC(36:5), PC(38:5), PC(34:1), PC(36:1), and TEI 9647 (Fig. S8) from online MS/MS analysis at the single cell level. Using the cell lysate, 12 species from the control group were further identified as PC(36:5), PC(34:1), PC(36:3), PC(38:6), PC(38:5), PC(38:4), PC(40:4), PC(38:7), TEI-9647, Coenzyme Q4, PC(40:6), and PC(40:7) (Fig. S9). Among them the first seven species were also detected in the lysate sample prepared using irinotecan treated cells (Fig. S10).

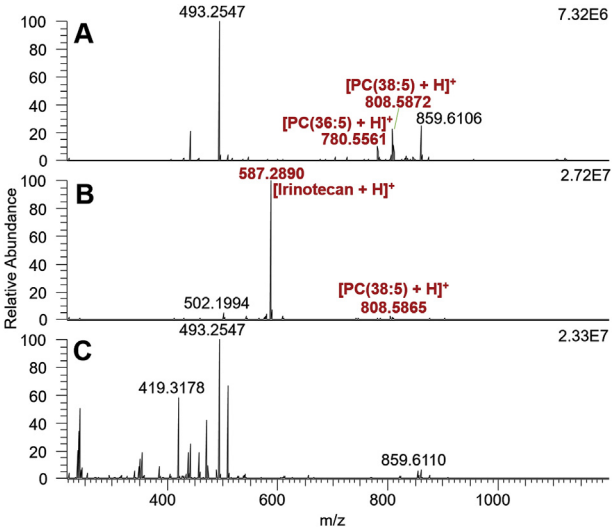

Fig. 3. Mass spectra of (A) a cell in the control group, (B) a cell in the drug treatment groups, and (C) background.

Interestingly, the antagonist of VDR (vitamin D_3 nuclear receptor), TEI-9647 [61–63], was only present in control cells. As previously reported vitamin D can hinder the progression of colon cancer [64,65] through its active form 1,25-dihydroxyvitamin D_3 (1,25D), which induces growth arrest and apoptosis of cancer cells [63]. Importantly, activating VDR in cancer cells is needed for the effective treatment using 1,25D [63,66]. Our experimental results can likely provide rationales to these observations in previous studies. Producing TEI-9647 seems to be a protection mechanism of cancer cells against their undesired chemical environment, and this antagonist can suppress the activity of VDR to disable the anticancer functions of 1,25D. The absence of TEI-9647 in cancer cells upon irinotecan treatment likely indicates this anticancer drug may hinder synthetic pathways of TEI-9647, which can potentially be a new mechanism in addition to its known inhibition function of topoisomerase [67]. However, comprehensive studies are still needed to verify our hypothesis.

3.3. Changes of metabolomic profiles after drug treatment

Lipid metabolism is regulated by several cellular processes including cell growth, proliferation, apoptosis, chemotherapy response, and drug resistance [68]. To illustrate the influence of anticancer drug treatment on cellular metabolism, we conducted statistical analysis of the SCMS data. Specifically, PLS-DA was conducted to illustrate the difference of overall metabolomic profiles between two groups of cells [69], followed by the permutation test to validate the results [70]. We then used *t*-test to compare metabolites' abundances before and after treatment. Intuitively, a visual discrimination of chemical profiles between two groups can be observed from the PLS-DA score plot (Fig. 4), and the corresponding permutation test indicates that the difference is statistically significant (p-value < 0.001). Through the *t*-test we discovered that a few types of lipids, including PC, PG, phosphatidylserine (PS), PE, and triglycerides (TG), were significantly changed (most of them were downregulated) due to drug treatment (Table S4). From a biological perspective, phosphatidic acid (PA) is the precursor for the biosynthesis of TGs and other phospholipids such as PC, PG, and PE [71,72]. The suppressed production of PA upon the exposure to irinotecan, which was also reported in other studies [73], can likely result in reduced synthesis of down-stream metabolites, such as TGs and phospholipids.

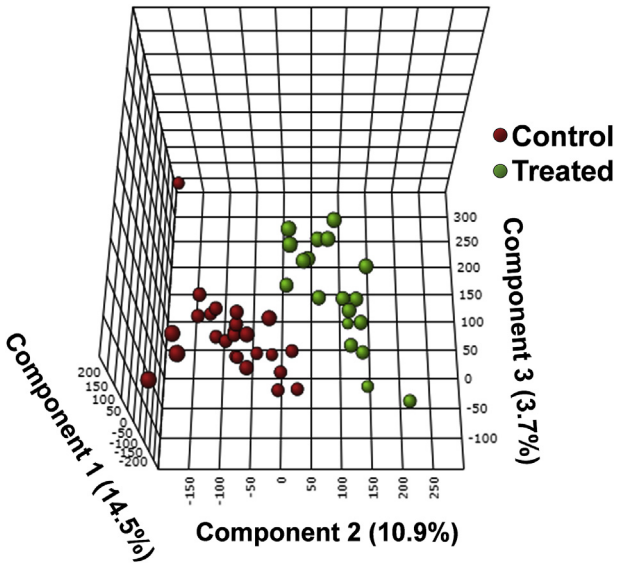

Fig. 4. 3D PLS-DA plot illustrating the metabolomic difference of cells between the control (red dots) and the treatment (green dots) groups. Each dot represents the overall metabolomic profile of a single cell. (For interpretation of the references to color in this figure legend, the reader is referred to the Web version of this article.)

In addition, a number of abundant species, including PE-Cer(d40:2) (*m/z* 781.5588) and SM(d37:1) (*m/z* 783.5758), were only detected from single cells rather than cell lysates (Tables S2 and S3), indicating that these cellular species are rapidly altered due to changes of cell microenvironment, or they are too labile to survive from multi-step sample preparation procedures. Due to the minimum sample preparation and rapid analysis, our technology allows for detection of cellular species reflecting the status of live cells with minimum perturbation of cell microenvironment.

4. Conclusion

We reported a redesigned T-probe that can be coupled to a mass spectrometer to conduct rapid, *in situ* SCMS analysis of entire live single cells in suspension. HCT-116 cell line was used as the model, and cells in control and drug treatment groups were subjected to the SCMS experiments. An individual cell was initially withdrawn into the probe, subsequently subjected to a rapid online lysis upon mixing with lysis solvent, and immediately ionized for real-time MS detection. The major advantage of this new design is that this device can be used to analyze non-adherent cells without cellular contents loss, as an entire cell is lysed inside the device. A variety of cellular species, including PC, PS, PE, PG, and TG, were detected from control and irinotecan treated single cells, with some of those further identified through online MS/MS analysis at the single cell level. Evident changes of metabolomic profiles of single cells after drug treatment were visualized through PLS-DA, and cellular species (i.e., PC, PG, PS, PE, and TG) with significant changes were discovered through *t*-test. In addition, we detected a number of species only present in single cells rather than cell lysates, indicating they are likely to be liable metabolites and sensitive to the change of cellular microenvironment. Our techniques can be potentially used for future SCMS analysis of broader range of non-adherent cell types with different sizes such as patient cells suspended in biological fluids.

Declaration of interests

The authors declare that they have no known competing financial interests or personal relationships that could have appeared to influence the work reported in this paper.

Acknowledgement

We acknowledge Dr. Steven B. Foster in the Mass Spectrometry Facility at the University of Oklahoma for providing invaluable expertise in LC-MS/MS experiments, and Wenhua Wang (University of Oklahoma) for assisting data analysis. This research project is partially supported by grants from National Institutes of Health (R01GM116116 and R21CA204706) and National Science Foundation (MRI-1626372 and OCE-1634630).

Appendix A. Supplementary data

Supplementary data to this article can be found online at https://doi.org/10.1016/j.aca.2019.07.059.

References

[1] Z. Liu, L.D. Lavis, E. Betzig, Imaging live-cell dynamics and structure at the single-molecule level, Mol. Cell 58 (4) (2015) 644–659.

[2] P. Rué, A.M. Arias, Cell dynamics and gene expression control in tissue homeostasis and development, Mol. Syst. Biol. 11 (2) (2015) 792.
[3] S.J. Altschuler, L.F. Wu, Cellular heterogeneity: do differences make a difference? Cell 141 (4) (2010) 559–563.
[4] K. Dettmer, P.A. Aronov, B.D. Hammock, Mass spectrometry-based metabolomics, Mass Spectrom. Rev. 26 (1) (2007) 51–78.
[5] C. Gawad, W. Koh, S.R. Quake, Single-cell genome sequencing: current state of the science, Nat. Rev. Genet. 17 (3) (2016) 175.
[6] I. Kanter, T. Kalisky, Single cell transcriptomics: methods and applications, Frontiers in oncology 5 (2015) 53.
[7] J.R. Newman, S. Ghaemmaghami, J. Ihmels, D.K. Breslow, M. Noble, J.L. DeRisi, J.S. Weissman, Single-cell proteomic analysis of S. cerevisiae reveals the architecture of biological noise, Nature 441 (7095) (2006) 840.
[8] S.S. Rubakhin, E.J. Lanni, J.V. Sweedler, Progress toward single cell metabolomics, Curr. Opin. Biotechnol. 24 (1) (2013) 95–104.
[9] R. Zenobi, Single-cell metabolomics: analytical and biological perspectives, Science 342 (6163) (2013) 1243259.
[10] X.-C. Zhang, Z.-W. Wei, X.-Y. Gong, X.-Y. Si, Y.-Y. Zhao, C.-D. Yang, S.-C. Zhang, X.-R. Zhang, Integrated droplet-based microextraction with ESI-MS for removal of matrix interference in single-cell analysis, Sci. Rep. 6 (2016) 24730.
[11] S.S. Rubakhin, E.V. Romanova, P. Nemes, J.V. Sweedler, Profiling metabolites and peptides in single cells, Nat. Methods 8 (4s) (2011) S20.
[12] Y. Yang, Y. Huang, J. Wu, N. Liu, J. Deng, T. Luan, Single-cell analysis by ambient mass spectrometry, Trac. Trends Anal. Chem. 90 (2017) 14–26.
[13] L. Zhang, A. Vertes, Single-cell mass spectrometry approaches to explore cellular heterogeneity, Angew. Chem. Int. Ed. 57 (17) (2018) 4466–4477.
[14] K.D. Duncan, J. Fyrestam, I. Lanekoff, Advances in mass spectrometry based single-cell metabolomics, Analyst 144 (3) (2018) 782–793.
[15] A.J. Ibáñez, S.R. Fagerer, A.M. Schmidt, P.L. Urban, K. Jefimovs, P. Geiger, R. Dechant, M. Heinemann, R. Zenobi, Mass spectrometry-based metabolomics of single yeast cells, Proc. Natl. Acad. Sci. 110 (22) (2013) 8790–8794.
[16] M.-Z. Huang, C.-H. Yuan, S.-C. Cheng, Y.-T. Cho, J. Shiea, Ambient ionization mass spectrometry, Annu. Rev. Anal. Chem. 3 (2010) 43–65.
[17] R.G. Cooks, Z. Ouyang, Z. Takats, J.M. Wiseman, Ambient mass spectrometry, Science 311 (5767) (2006) 1566–1570.
[18] M.E. Monge, G.A. Harris, P. Dwivedi, F.M. Fernández, Mass spectrometry: recent advances in direct open air surface sampling/ionization, Chem. Rev. 113 (4) (2013) 2269–2308.
[19] N. Tsuyama, H. Mizuno, E. Tokunaga, T. Masujima, Live single-cell molecular analysis by video-mass spectrometry, Anal. Sci. 24 (5) (2008) 559–561.
[20] B. Shrestha, A. Vertes, In situ metabolic profiling of single cells by laser ablation electrospray ionization mass spectrometry, Anal. Chem. 81 (20) (2009) 8265–8271.
[21] H.-M. Bergman, I. Lanekoff, Profiling and quantifying endogenous molecules in single cells using nano-DESI MS, Analyst 142 (19) (2017) 3639–3647.
[22] H. Zhu, G. Zou, N. Wang, M. Zhuang, W. Xiong, G. Huang, Single-neuron identification of chemical constituents, physiological changes, and metabolism using mass spectrometry, Proc. Natl. Acad. Sci. (2017) 201615557.
[23] X. Gong, Y. Zhao, S. Cai, S. Fu, C. Yang, S. Zhang, X. Zhang, Single cell analysis with probe ESI-mass spectrometry: detection of metabolites at cellular and subcellular levels, Anal. Chem. 86 (8) (2014) 3809–3816.
[24] F. Chen, L. Lin, J. Zhang, Z. He, K. Uchiyama, J.-M. Lin, Single-cell analysis using drop-on-demand inkjet printing and probe electrospray ionization mass spectrometry, Anal. Chem. 88 (8) (2016) 4354–4360.
[25] S. Mao, W. Zhang, Q. Huang, M. Khan, H. Li, K. Uchiyama, J.M. Lin, In situ scatheless cell detachment reveals correlation between adhesion strength and viability at single-cell resolution, Angew. Chem. Int. Ed. 57 (1) (2018) 236–240.
[26] M.C. Naill, S.C. Roberts, Flow cytometric analysis of protein content in Taxus protoplasts and single cells as compared to aggregated suspension cultures, Plant Cell Rep. 23 (8) (2005) 528–533.
[27] D.R. Bandura, V.I. Baranov, O.I. Ornatsky, A. Antonov, R. Kinach, X. Lou, S. Pavlov, S. Vorobiev, J.E. Dick, S.D. Tanner, Mass cytometry: technique for real time single cell multitarget immunoassay based on inductively coupled plasma time-of-flight mass spectrometry, Anal. Chem. 81 (16) (2009) 6813–6822.
[28] N. Pan, W. Rao, N.R. Kothapalli, R. Liu, A.W. Burgett, Z. Yang, The single-probe: a miniaturized multifunctional device for single cell mass spectrometry analysis, Anal. Chem. 86 (19) (2014) 9376–9380.
[29] W. Rao, N. Pan, Z. Yang, Applications of the single-probe: mass spectrometry imaging and single cell analysis under ambient conditions, J. Vis. Exp.: J. Vis. Exp. 112 (2016) 539111.
[30] M. Sun, Z. Yang, B. Wawrik, Metabolomic fingerprints of individual algal cells using the single-probe mass spectrometry technique, Front. Plant Sci. 9 (2018) 571.
[31] R. Liu, G. Zhang, Z. Yang, Towards rapid prediction of drug-resistant cancer cell phenotypes: single cell mass spectrometry combined with machine learning, Chem. Commun. 55 (5) (2019) 616–619.
[32] X. Tian, G. Zhang, Y. Shao, Z. Yang, Towards enhanced metabolomic data analysis of mass spectrometry image: multivariate Curve Resolution and Machine Learning, Anal. Chim. Acta 1037 (2018) 211–219.
[33] X. Tian, G. Zhang, Z. Zou, Z. Yang, Anticancer drug affects metabolomic profiles in multicellular spheroids: studies using mass spectrometry imaging combined with machine learning, Anal. Chem. 91 (9) (2019) 5802–5809.
[34] W. Rao, N. Pan, X. Tian, Z. Yang, High-resolution ambient MS imaging of negative ions in positive ion mode: using dicationic reagents with the single-probe, J. Am. Soc. Mass Spectrom. 27 (1) (2016) 124–134.
[35] M. Sun, X. Tian, Z. Yang, Microscale mass spectrometry analysis of extracellular metabolites in live multicellular tumor spheroids, Anal. Chem. 89 (17) (2017) 9069–9076.
[36] R. Liu, N. Pan, Y. Zhu, Z. Yang, T-Probe, An integrated microscale device for online in situ single cell analysis and metabolic profiling using mass spectrometry, Anal. Chem. 90 (18) (2018) 11078–11085.
[37] T. Masujima, Live single-cell mass spectrometry, Anal. Sci. 25 (8) (2009) 953–960.
[38] D.A. Carter, K.E. Fernandes, A. Brockway, M. Haverkamp, C.A. Cuomo, F. Van Ogtrop, J.R. Perfect, Phenotypic variability correlates with clinical outcome in Cryptococcus isolates obtained from Botswanan HIV/AIDS patients, BioRxiv (2018) 418897.
[39] R.M. Onjiko, E.P. Portero, S.A. Moody, P. Nemes, In situ microprobe single-cell capillary electrophoresis mass spectrometry: metabolic reorganization in single differentiating cells in the live vertebrate (Xenopus laevis) embryo, Anal. Chem. 89 (13) (2017) 7069–7076.
[40] L. Sun, M.M. Bertke, M.M. Champion, G. Zhu, P.W. Huber, N.J. Dovichi, Quantitative proteomics of Xenopus laevis embryos: expression kinetics of nearly 4000 proteins during early development, Sci. Rep. 4 (2014) 4365.
[41] L. Sun, K.M. Dubiak, E.H. Peuchen, Z. Zhang, G. Zhu, P.W. Huber, N.J. Dovichi, Single cell proteomics using frog (Xenopus laevis) blastomeres isolated from early stage embryos, which form a geometric progression in protein content, Anal. Chem. 88 (13) (2016) 6653–6657.
[42] R. Cumeras, E. Figueras, C. Davis, J.I. Baumbach, I. Gracia, Review on ion mobility spectrometry. Part 1: current instrumentation, Analyst 140 (5) (2015) 1376–1390.
[43] L. Zhang, D.P. Foreman, P.A. Grant, B. Shrestha, S.A. Moody, F. Villiers, J.M. Kwak, A. Vertes, In Situ metabolic analysis of single plant cells by capillary microsampling and electrospray ionization mass spectrometry with ion mobility separation, Analyst 139 (20) (2014) 5079–5085.
[44] C. Lombard-Banek, S.A. Moody, P. Nemes, Single-cell mass spectrometry for discovery proteomics: quantifying translational cell heterogeneity in the 16-cell frog (Xenopus) embryo, Angew. Chem. Int. Ed. 55 (7) (2016) 2454–2458.
[45] W.G. Lewis, Z. Shen, M. Finn, G. Siuzdak, Desorption/ionization on silicon (DIOS) mass spectrometry: background and applications, Int. J. Mass Spectrom. 226 (1) (2003) 107–116.
[46] L. Mazutis, J. Gilbert, W.L. Ung, D.A. Weitz, A.D. Griffiths, J.A. Heyman, Single-cell analysis and sorting using droplet-based microfluidics, Nat. Protoc. 8 (5) (2013) 870.
[47] F. Pierigè, N. Bigini, L. Rossi, M. Magnani, Reengineering red blood cells for cellular therapeutics and diagnostics, Wiley.Interdiscip.Rev.: Nanomed.Nanobiotechnol. 9 (5) (2017) e1454.
[48] J.-C. Liao, Cell therapy using bone marrow-derived stem cell overexpressing BMP-7 for degenerative discs in a rat tail disc model, Int. J. Mol. Sci. 17 (2) (2016) 147.
[49] P. Potdar, N. Lotey, Role of circulating tumor cells in future diagnosis and therapy of cancer, J. Cancer. Metastasis.Treat 1 (2) (2015), 44-44.
[50] S.P. Weisberg, M. Chang, P. Muranski, D. Farber, Efficient expansion of polyfunctional virus-specific T cells from human lymph nodes: implications for cellular therapies, Blood 132 (2018) 3751.
[51] S.J. Standke, D.H. Colby, R.C. Bensen, A.W. Burgett, Z. Yang, Mass spectrometry measurement of single suspended cells using a combined cell manipulation system and a single-probe device, Anal. Chem. 91 (3) (2019) 1738–1742.
[52] N. Pan, W. Rao, S.J. Standke, Z. Yang, Using dicationic ion-pairing compounds to enhance the single cell mass spectrometry analysis using the single-probe: a microscale sampling and ionization device, Anal. Chem. 88 (13) (2016) 6812–6819.
[53] E.L. Beard Jr., The american society of health system pharmacists, JONA's Healthc. Law, Ethics, Regul. 3 (3) (2001) 78–79.
[54] E. Gupta, R. Mick, J. Ramirez, X. Wang, T.M. Lestingi, E.E. Vokes, M.J. Ratain, Pharmacokinetic and pharmacodynamic evaluation of the topoisomerase inhibitor irinotecan in cancer patients, J. Clin. Oncol. 15 (4) (1997) 1502–1510.
[55] I. Lanekoff, B.S. Heath, A. Liyu, M. Thomas, J.P. Carson, J. Laskin, Automated platform for high-resolution tissue imaging using nanospray desorption electrospray ionization mass spectrometry, Anal. Chem. 84 (19) (2012) 8351–8356.
[56] R. Liu, G. Zhang, M. Sun, X. Pan, Z. Yang, Integrating a generalized data analysis workflow with the single-probe mass spectrometry experiment for single cell metabolomics, Anal. Chim. Acta 1064 (2019), 71-7915.
[57] J. Xia, D.S. Wishart, Using MetaboAnalyst 3.0 for comprehensive metabolomics data analysis, Current protocols in bioinformatics 55 (1) (2016) 14, 10.1-14.10.91.
[58] P.S. Gromski, H. Muhamadali, D.I. Ellis, Y. Xu, E. Correa, M.L. Turner, R. Goodacre, A tutorial review: metabolomics and partial least squares-discriminant analysis–a marriage of convenience or a shotgun wedding, Anal. Chim. Acta 879 (2015) 10–23.
[59] C.A. Smith, G. O'Maille, E.J. Want, C. Qin, S.A. Trauger, T.R. Brandon, D.E. Custodio, R. Abagyan, G. Siuzdak, METLIN: a metabolite mass spectral database, Ther. Drug Monit. 27 (6) (2005) 747–751.
[60] D.S. Wishart, T. Jewison, A.C. Guo, M. Wilson, C. Knox, Y. Liu, Y. Djoumbou, R. Mandal, F. Aziat, E. Dong, HMDB 3.0—the human metabolome database in 2013, Nucleic Acids Res. 41 (D1) (2012) D801–D807.
[61] S. Ishizuka, N. Kurihara, D. Miura, K. Takenouchi, J. Cornish, T. Cundy,

S.V. Reddy, G.D. Roodman, Vitamin D antagonist, TEI-9647, inhibits osteoclast formation induced by 1α, 25-dihydroxyvitamin D3 from pagetic bone marrow cells, J. Steroid Biochem. Mol. Biol. 89 (2004) 331–334.
[62] M. Peräkylä, F. Molnár, C. Carlberg, A structural basis for the species-specific antagonism of 26, 23-lactones on vitamin D signaling, Chem. Biol. 11 (8) (2004) 1147–1156.
[63] F. Pereira, M.J. Larriba, A. Muñoz, Vitamin D and colon cancer, Endocr. Relat. Cancer 19 (3) (2012) R51–R71.
[64] C.F. Garland, F.C. Garland, Do sunlight and vitamin D reduce the likelihood of colon cancer? Int. J. Epidemiol. 9 (3) (1980) 227–231.
[65] J.M. Lappe, D. Travers-Gustafson, K.M. Davies, R.R. Recker, R.P. Heaney, Vitamin D and calcium supplementation reduces cancer risk: results of a randomized trial, Am. J. Clin. Nutr. 85 (6) (2007) 1586–1591.
[66] S. Shah, M.N. Islam, S. Dakshanamurthy, I. Rizvi, M. Rao, R. Herrell, G. Zinser, M. Valrance, A. Aranda, D. Moras, The molecular basis of vitamin D receptor and β-catenin crossregulation, Mol. Cell 21 (6) (2006) 799–809.
[67] R.H. Mathijssen, W.J. Loos, J. Verweij, A. Sparreboom, Pharmacology of topoisomerase I inhibitors irinotecan (CPT-11) and topotecan, Curr. Cancer Drug Targets 2 (2) (2002) 103–123.
[68] C. Huang, C. Freter, Lipid metabolism, apoptosis and cancer therapy, Int. J. Mol. Sci. 16 (1) (2015) 924–949.
[69] J.A. Westerhuis, H.C. Hoefsloot, S. Smit, D.J. Vis, A.K. Smilde, E.J. van Velzen, J.P. van Duijnhoven, F.A. van Dorsten, Assessment of PLSDA cross validation, Metabolomics 4 (1) (2008) 81–89.
[70] P. Golland, B. Fischl, Permutation tests for classification: towards statistical significance in image-based studies, in: Biennial International Conference on Information Processing in Medical Imaging, Springer, 2003, pp. 330–341.
[71] A. Sreenivas, M.J. Villa-Garcia, S.A. Henry, G.M. Carman, Phosphorylation of the yeast phospholipid synthesis regulatory protein Opi1p by protein kinase C, J. Biol. Chem. 276 (32) (2001) 29915–29923.
[72] L.-S. Hsieh, W.-M. Su, G.-S. Han, G.M. Carman, Phosphorylation regulates the ubiquitin-independent degradation of yeast Pah1 phosphatidate phosphatase by the 20S proteasome, J. Biol. Chem. 290 (18) (2015) 11467–11478.
[73] C. Blandizzi, B. De Paolis, R. Colucci, G. Lazzeri, F. Baschiera, M. Del Tacca, Characterization of a novel mechanism accounting for the adverse cholinergic effects of the anticancer drug irinotecan, Br. J. Pharmacol. 132 (1) (2001) 73–84.